ANALYSIS OF FLOOD AND RIVER BED VARIATION IN THE KAMANASHI RIVER WITH LARGE AMOUNT OF SEDIMENT DEPOSITION

SHIRO OKAYAMA
Civil, Human and Environmental Engineering, Chuo University, Tokyo, Japan, a15.4b5c@g.chuo-u.ac.jp

YUKO NAITO
Kofu River and Road Office, Kanto Regional Development Bureau, Ministry of Land, Infrastructure, Transport and Tourism, Yamanashi, Japan, naitou-y8311@mlit.go.jp

SHOJI FUKUOKA
Research and Development Initiative, Chuo University, Tokyo, Japan, sfuku@tamacc.chuo-u.ac.jp

GOTOH TAKAHISA
Research and Development Initiative, Chuo University, Tokyo, Japan, goto510@tamacc.chuo-u.ac.jp

ABSTRACT
The Kamanashi River is a steep river with gravel grains, cobbles and boulders. In 1982, the record breaking largest flood occurred and the large amount of sediments yielding in the upstream mountainous area flowed into and deposited in the river channels. The depositions mainly occurred in the lower reaches where the bed slope was milder than the upper reaches. In addition, the grain size distributions became coarser in the upper reaches and finer in the lower reaches due to sorting during the flood. In this study, we developed and applied flood flow and bed variation analysis method considering the non-equilibrium sediment motions of boulders and gravel grains with large amount of suspended sediments for the 1982 flood. The upstream boundary condition of the bed variation analysis was given by estimating the large amount of sediment discharge from the upstream mountainous area. The calculation results clarified the process of the particle distributions fining in the lower reach and the process of the one becoming coarser in the upper reach. And the calculation results demonstrated the tendency of the deposition shown in the observed data in the lower reach after the flood.

Keywords: *non-equilibrium flow and sediment, upper sediment boundary condition, a large amount of sediments yields, flood flow, bed variation*

1. INTRODUCTION

The Kamanashi River is a steep river with gravel grains, cobbles and boulders. The well developed double-row bars are formed as shown in Figure 1(a). In August 1982, the record breaking largest flood occurred and a large amount of sediment yields occurred in the upstream mountainous area. The large amount of sediment yields brought large-scale sediment depositions and channel migrations of the double-row bars as shown in Figure 1(b). In addition, the grain size distributions after the flood became coarser in the upper reaches and finer in the lower reaches compared to those before the flood due to sorting (Ikeda et.al., 1986 and Parker, 1991).

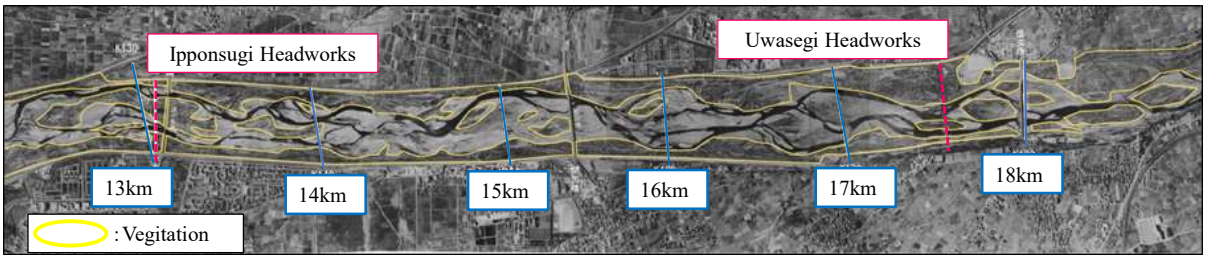

Figure 1(a). Aerial photograph before the flood

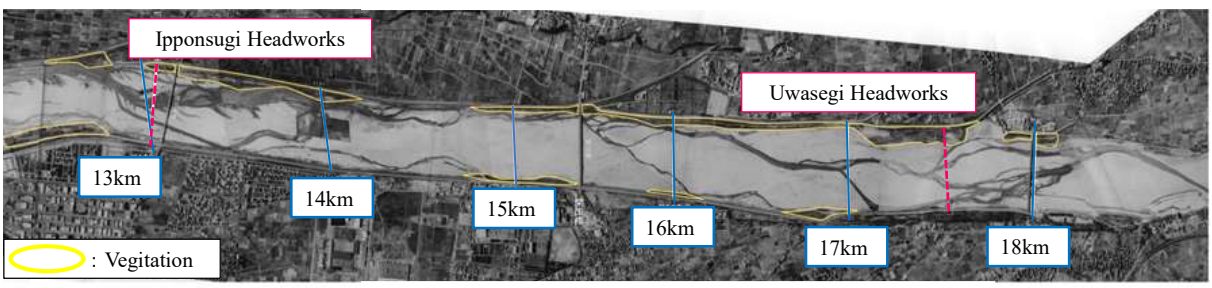

Figure 1(b). Aerial photograph after the flood

Parker proposed the bed variation analysis method considering selective sorting and abrasion. The bed load discharge was calculated by using the equilibrium bed load transport equation in his study. He applied and predicted the long term changes in riverbed gradients and the downstream sediments fining under conditions of near the bunkfull discharge. However, it is necessary to consider the non-equilibrium sediment motions in order to calculate the large amount of sediment depositions due to active motions of gravel grains in the Kamanashi River. The objective of the study is to develop the flood flow and bed variation analysis method considering the non-equilibrium sediment motions in the gravel bed rivers containing large amount of suspended sediment transports. In addition, we investigate the mechanism of large-scale sediment depositions and sorting of bed materials due to 1982 flood of the Kamanashi River by applying the developed method of bed variation analysis.

2. LONGITUDINAL SEDIMENTATION AND SORTING CAUSED BY THE 1982 FLOOD

Figure 2 shows longitudinal distributions of the flood marks and the measured mean bed elevations before and after the flood. Flood marks rose to around the designed water levels. In the downstream from 10km point, the water surface profiles became mild due to the backwater from the Unose contraction reaches and the confluence of the Fuefuki River.

Figure 3 indicates the measured longitudinal distributions of sediment depositions after the flood. The 1982 flood caused the large amount of sediment yields in the upstream mountainous area and most of those sediments flowed into the river channel. The amount of sediment depositions in the objective reaches were approximately 2 million m^3 as shown in Figure 3. And the large-scale sediment depositions tended to occur in the lower reaches (14km to 5km) where the bed slope was milder than the upper reaches.

Figure 4 shows the grain size distributions of bed materials in the objective reaches before and after the flood. The shape of grain size distributions before the flood was almost same shape for longitudinal directions, and size of D60 was about 20mm. However, the grain size distributions after the flood became coarser in the upper reaches (24km ~ 20km) and became finer in the lower reaches (14km to 5km). The mean size of D60 in upper reaches became 100mm and that in the lower reaches became 3mm. These facts indicated that the coarse sediments deposited in the upper reaches and the fine sediments were transported to the lower reaches during the large flood.

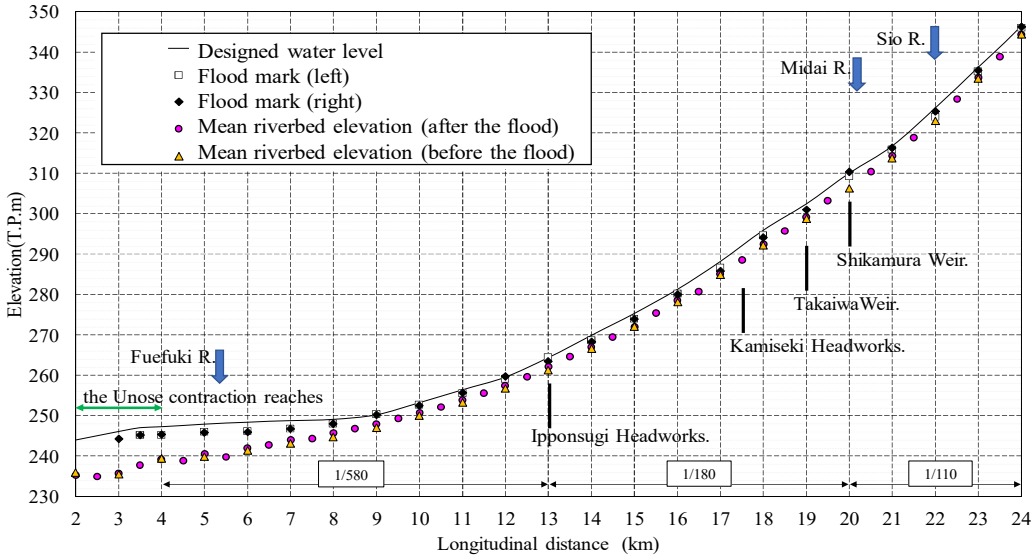

Figure 2. Longitudinal distributions of the flood marks and measured mean bed elevations before and after the flood

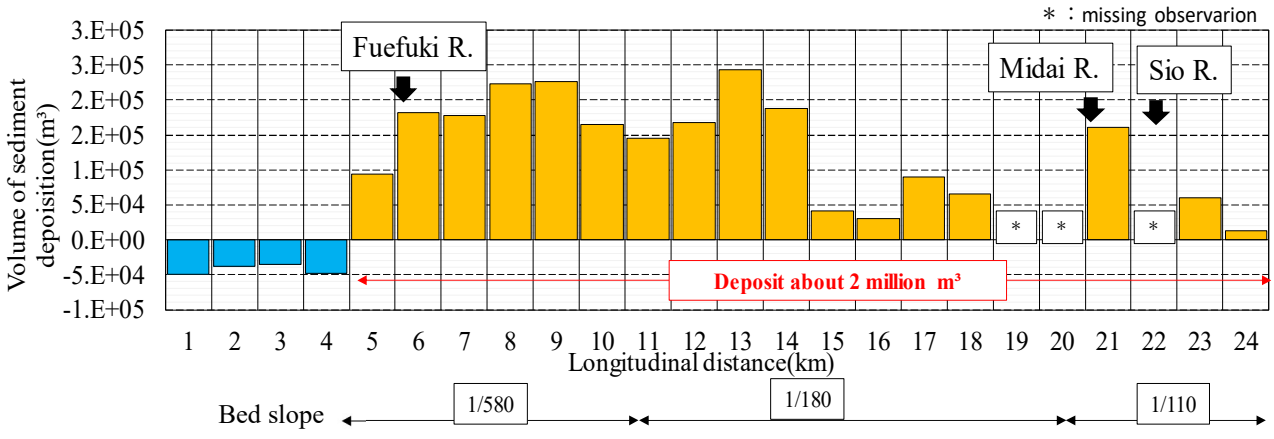

Figure 3. Measured longitudinal distributions of sediment depositions after the flood

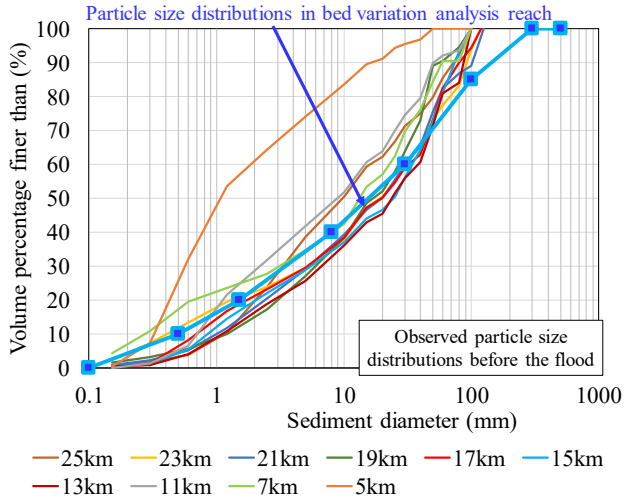

Figure 4(a) the grain size distributions around bed surface material before the flood

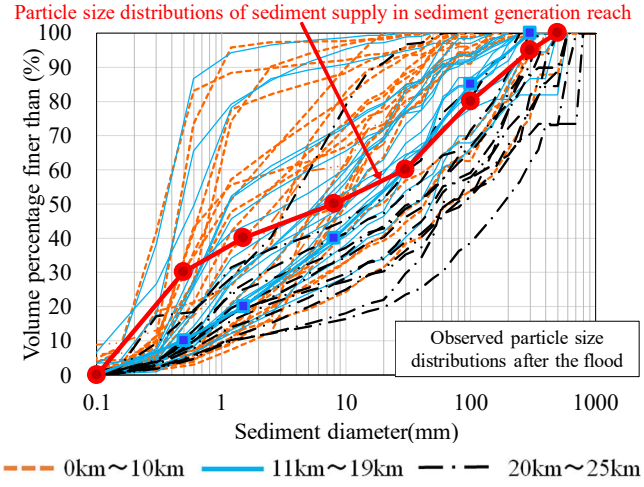

Figure 4(b) the grain size distributions around bed surface material after the flood

3. ANALYSIS METHOD AND CONDITIONS

3.1 Analysis method

In this study, the quasi-three-dimensional flow analysis method (Q3D-FEBS method, Takemura & Fukuoka, 2019) was applied in order to accurately calculate flood flows and bed variations in the Kamanashi River with the double-row bars. The Q3D-FEBS method was able to calculate the three-dimensional velocity distributions and pressure distributions in the framework of the depth integrated model. The velocity distributions in the vertical direction were determined by the equations of motion on a water surface ($\eta = 0$) and a bottom surface ($\eta = 1$) shown in Eq.(3) and Eq.(4) in addition to the depth-integrated continuity equations and the momentum equations shown in Eq. (1) and Eq. (2). The elevation of bottom surface was defined as slightly higher than the bed surface. ($z_b = \delta z_b + z_0, \delta z_b = c_{zb}h, c_{zb} = 0.03$)

$$\frac{\partial h}{\partial t} + \frac{\partial U_j h}{\partial x_j} = 0 \tag{1}$$

$$\frac{\partial U_i h}{\partial t} + \frac{\partial U_i U_j h}{\partial x_j} = -gh\frac{\partial z_s}{\partial x_i} - \frac{1}{\rho}\frac{\partial h\overline{p'}}{\partial x_i} - \frac{p'_b}{\rho}\frac{\partial z_b}{\partial x_i} - \frac{\partial h\overline{u'_i u'_j}}{\partial x_j} + \frac{\partial}{\partial x_j}\nu_t h\left(\frac{\partial U_i}{\partial x_j} + \frac{\partial U_j}{\partial x_i}\right) - \hat{S}\frac{\hat{\tau}_{bi}}{\rho} \tag{2}$$

$$\frac{\partial u_{si}}{\partial t} + u_{sj}\frac{\partial u_{si}}{\partial x_j} = -g\frac{\partial z_s}{\partial x_i} + \frac{1}{\rho}\frac{\partial p'}{\partial z}\bigg|_s\frac{\partial z_s}{\partial x_i} + \frac{\nu_{ts}}{\rho}\frac{\partial^2 u_i}{\partial z^2}\bigg|_s \tag{3}$$

$$\frac{\partial u_{bi}}{\partial t} + u_{bj}\frac{\partial u_{bi}}{\partial x_j} = -g\frac{\partial z_s}{\partial x_i} - \frac{1}{\rho}\frac{\partial p'_b}{\partial x_i} + \frac{1}{\rho}\frac{\partial p'}{\partial z}\bigg|_b\frac{\partial z_b}{\partial x_i} + \frac{\partial}{\partial x_j}\nu_{tb}\left(\frac{\partial u_{bi}}{\partial x_j} + \frac{\partial u_{bj}}{\partial x_i}\right) + \frac{\hat{S}}{\rho}\frac{\hat{\tau}_{bi} - \hat{\tau}_{0i}}{\delta z_b} \tag{4}$$

$$u_i(\eta) = \Delta u_i(12\eta^3 - 12\eta^2 + 1) + \delta u_i(-4\eta^3 + 3\eta^2) + U_i \tag{5}$$

where, $i = 1, 2$ $(x_1 = x, x_2 = y)$, $u_i(\eta)$: velocity in i direction at any height, U_i: depth-average velocity in i direction, u_{si}: water surface velocity in i direction, u_{bi}: bottom surface velocity in i direction, $\Delta u_i = u_{si} - U_i$, $\delta u_i = u_{si} - u_{bi}$, z_s: water level, h: water depth, ρ: density of water, $u'_i = u_i - U_i$, g: acceleration of gravity, p': non-hydrostatic pressure, ν_t:kinetic eddy viscosity coefficient, $\hat{\tau}_{bi}$: shear stress acting on the height of bottom surface velocity in i direction, $\hat{S} = \sqrt{1 + (\partial z_b/\partial x_i)^2}$, $\hat{\tau}_{0i}$: shear stress acting on the bed surface in i direction. Overbar"–" represents a depth-averaged value.

The consideration of non-equilibrium sediment motions with a wide range of grain sizes from coarse to fine sediments was important for calculating large-scale sediment depositions and sorting. Therefore, we developed bed variation analysis method for stony and gravel bed rivers (Osada et.al., 2013) considering suspended sediment transports. The temporal changes in the volume of bed load were obtained from continuity equations of bed load in Eq. (6). The sediment discharge per unit was calculated by the volume of bed load and sediment particle velocity in Eq. (7), and the particle velocity was calculated from the saltation analysis (Osada et.al., 2013) using equations of motion of a sand particle in Eq. (8). The temporal changes in the height of each particle size was calculated by pick-up rate and deposit rate in Eq. (9). The deposit rate was calculated by the volume of bed load and the average moving period in Eq. (10). The average moving period T_{sal} was estimated by the saltation analysis of each particles. The pick-up rate was obtained from Eq. (11) by calculating the time T_{pick} required for pick up from river bed (Osada et.al., 2013). The equation of pick-up rate in Eq. (11) took into account the unevenness distributions of the riverbed elevations composed of each size of particles. Thereby, this method was able to calculate the shielding effects of coarse sediments on fine sediments (Osada et.al., 2013).

The transport of suspended sediments was calculated by horizontal 2D advection-diffusion equations in Eq. (12). The suspended sediment entrainments V_{suk} from the bed load motion was calculated by the particle velocity in the vertical direction in Eq. (13). The particle velocity in vertical direction was estimated by the equation of motion of the particle considering the effects of velocity fluctuations by turbulences in Eq. (14). The depositions were calculated from the falling velocity and the suspended sediment concentration near the bed.

$$\frac{\partial V_k}{\partial t} + \frac{\partial q_{bkj}}{\partial x_j} = -V_{bdk} + V_{bpk} - V_{suk} + V_{sdk} \tag{6}$$

$$q_{bkj} = u_{pkj} V_k \tag{7}$$

$$A_3(\rho_s + \rho C_M) d_k^3 \frac{\partial u_{pki}}{\partial t} = \frac{1}{2}\rho C_D A_2 d_k^2 (u_{bi} - u_{pki})|\boldsymbol{u}_b - \boldsymbol{u}_{pk}| - (\rho_s - \rho) A_3 d_k^3 g_i \tag{8}$$

$$\frac{\partial z_{bk}}{\partial t} = -\frac{A_2}{A_3}(V_{bpk} - V_{bdk}) \tag{9}$$

$$V_{bdk} = \frac{1}{t_{sal}} V_k \tag{10}$$

$$V_{bpk} = \varepsilon_p \left(\frac{p_k}{A_2 d_k^2}\right)\left(\frac{A_3 d_k^3}{T_{pick}}\right),\ \varepsilon_{pk} = 0.016 \tag{11}$$

$$\frac{\partial C_{sk} h}{\partial t} + \frac{\partial C_{sk} Uh}{\partial x} + \frac{\partial C_{sk} Vh}{\partial y} = \frac{\partial}{\partial x}\left(\nu_t h \frac{\partial C_{sk}}{\partial x}\right) + \frac{\partial}{\partial y}\left(\nu_t h \frac{\partial C_{sk}}{\partial y}\right) + V_{suk} - V_{sdk} \tag{12}$$

$$V_{suk} = C_{bk} w_{pk} \tag{13}$$

$$\begin{aligned} A_3(\rho_s + C_M)\rho d_k^3 \frac{dw_{pk}}{dt} &= F_z + F'_{zk} - A_3(\rho_s - \rho) g d_k^3 \\ = \frac{1}{2} A_2 d_k^2 C_d \rho (\overline{w_b} + w'_b - w_{pk}) &\sqrt{(\overline{u_b} + u'_b - u_{pk})^2 + (\overline{v_b} + v'_b - v_{pk})^2 + (\overline{w_b} + w'_b - w_{pk})^2} \\ -A_3(\rho_s - \rho) g_z d_k^3 & \end{aligned} \tag{14}$$

where, V_k : volume of bed load, q_{bi} : sediment discharge per unit width in i direction, V_{bdk} : deposition rate, V_{bpk} : pick-up rate, u_{pi} : particle velocity in i direction, ρ_s: gravel particle density, k : particle numbers, d_k : particle diameter, A_2 and A_3 : a two-dimensional and three-dimensional shape factor (=$\pi/4$, $\pi/6$), respectively, w_{pk}: vertical particle velocities, F'_z: the fluid forces generated by turbulence, F_z : fluid forces by mean flow velocities near the bottom.

3.2 Calculation conditions

Figure 5 shows the objective area and the locations of boundary conditions.The tributaries which were the Shio River, the Midai Rver, the Fuefuki River and the Ashi River were taken into account in the calculations. The upstream boundary condition of flood flow in each rivers was given by the discharge hydrographs obtained from the runoff analysis. The downstream boundary condition was given by observed water level hydrograph at Shimizubata observation station (2.7k) shown in Figure 6.

A large amount of inflow sediment discharge graph from the upstream mountainous basin during the flood should be taken into account as the upstream boundary condition of bed variation analysis of the Kamanasi River and the tributaries. The determination method of the inflow sediment discharge graph of these rivers was explained below. Figure 7 shows schematic diagram determining the upstream boundary conditions for bed variation analysis. It was assumed that the inflow sediment discharge of each particle sizes from the upper reaches was produced by sediment entrainments due to flood flows in the sediment generation reach (see Figure

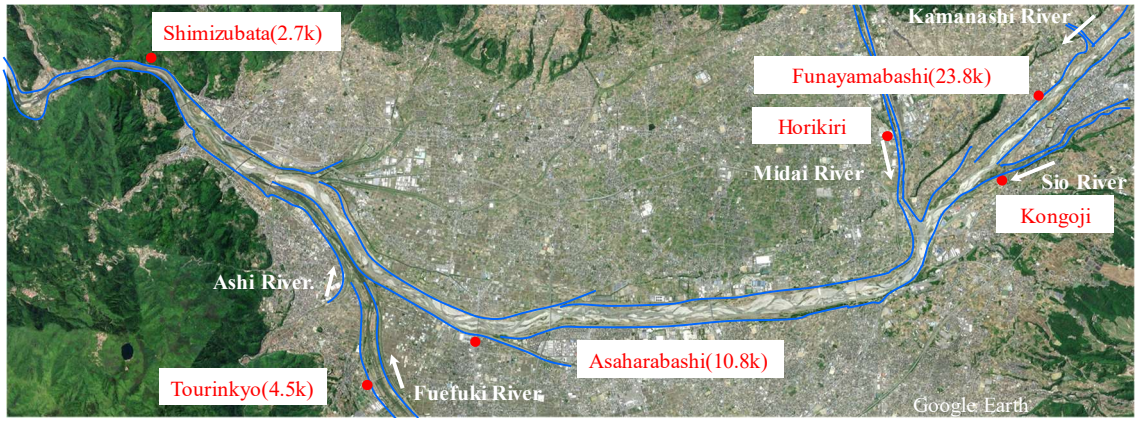

Figure 5. The analysis reach

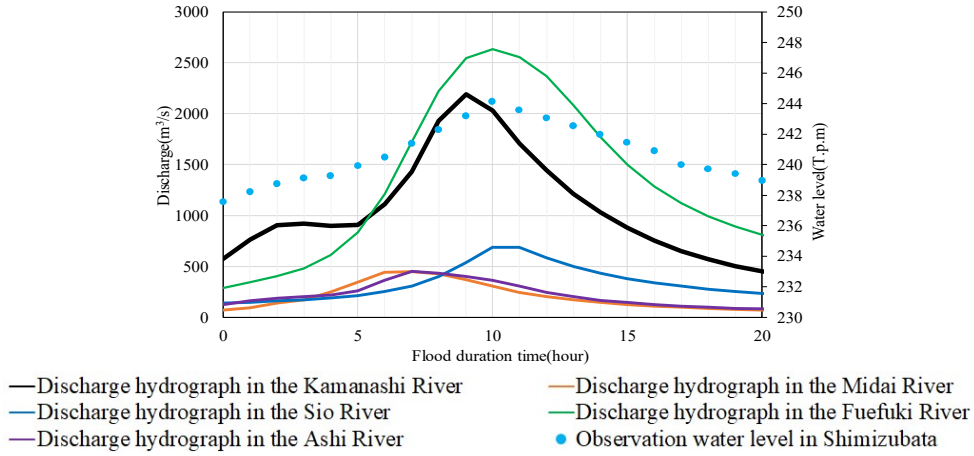

Figure 6. discharge hydrographs and observed water level of Shimizubata (2.7k)

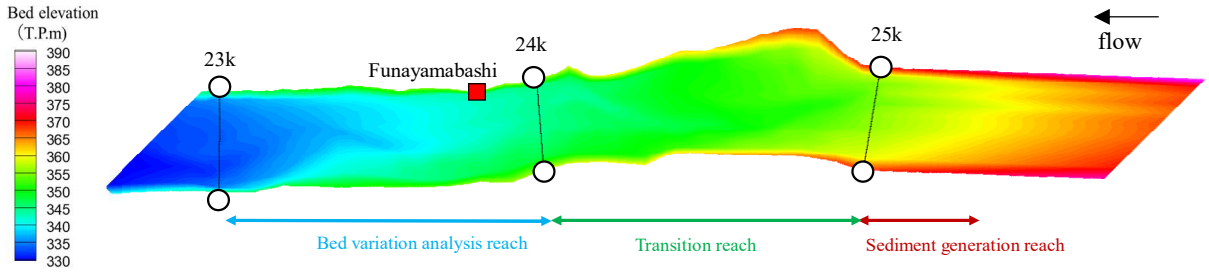

Figure 7. Calculation method of upstream boundary condition for the bed variation analysis

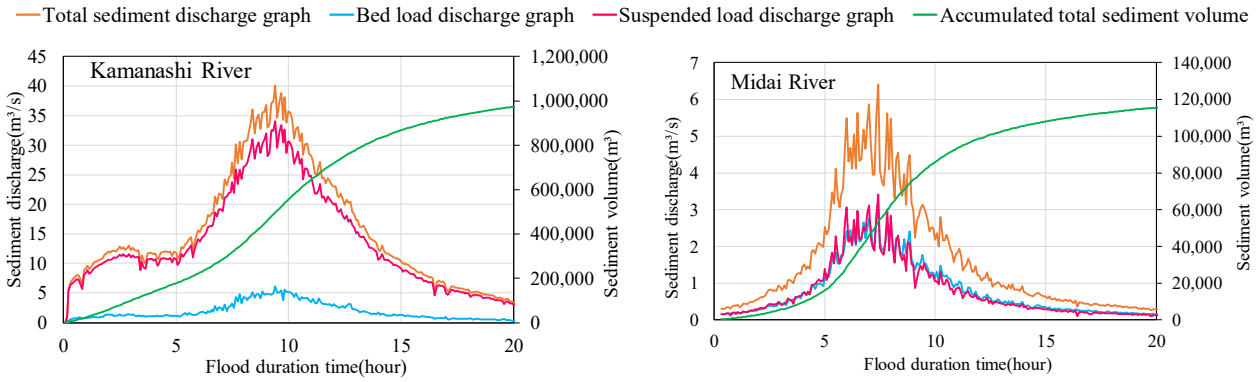

Figure 8(a). Sediment graph of the Kamanashi River

Figure (8b). Sediment graph of the Midai River

7) so as to agree with the observed bed variation and bed material distributions in the downstream reach. The bed gradients and channel widths in these reaches were given by the average channel width and bed slope around 25km point. The grain size distribution in the sediment generation reach was set so as to contain the fine sediment observed in the lower reach and the coarse sediment observed in the upper reach after the flood as shown in Figure 4(b).

The initial grain size distributions in the bed variation analysis are given based on the grain size distribution before the flood shown in Figure 4 (a). The transition reach was set between the sediment generation reach and the bed variation analysis reach. The sediment discharge graphs containing bed load and suspended load were formed in the transition reach and introduced as the upstream boundary condition of the bed variation analysis in the downstream.

Figures 8(a) and 8(b) show the sediment graphs of the Kamanashi River and the Midai River given as the boundary conditions of upstream end. The shape of the sediment graph was assumed to be similar to that of the discharge hydrograph. About 1,000,000 m^3 of sediment flowed into from the Kamanashi River, and about 120,000 m^3 from the Midai River.

4. ANALYSIS RESULTS

Figure 9 shows the distribution of flood marks, calculated water surface profiles, the observed and calculated mean bed elevations before and after the flood. The calculated water surface profiles at 9hours(peak time) explained the observed water surface profile that was raised due to the Unose contraction reach and the confluence of the Fuefuki River, although it was higher than the flood marks in the reach between 24 km and

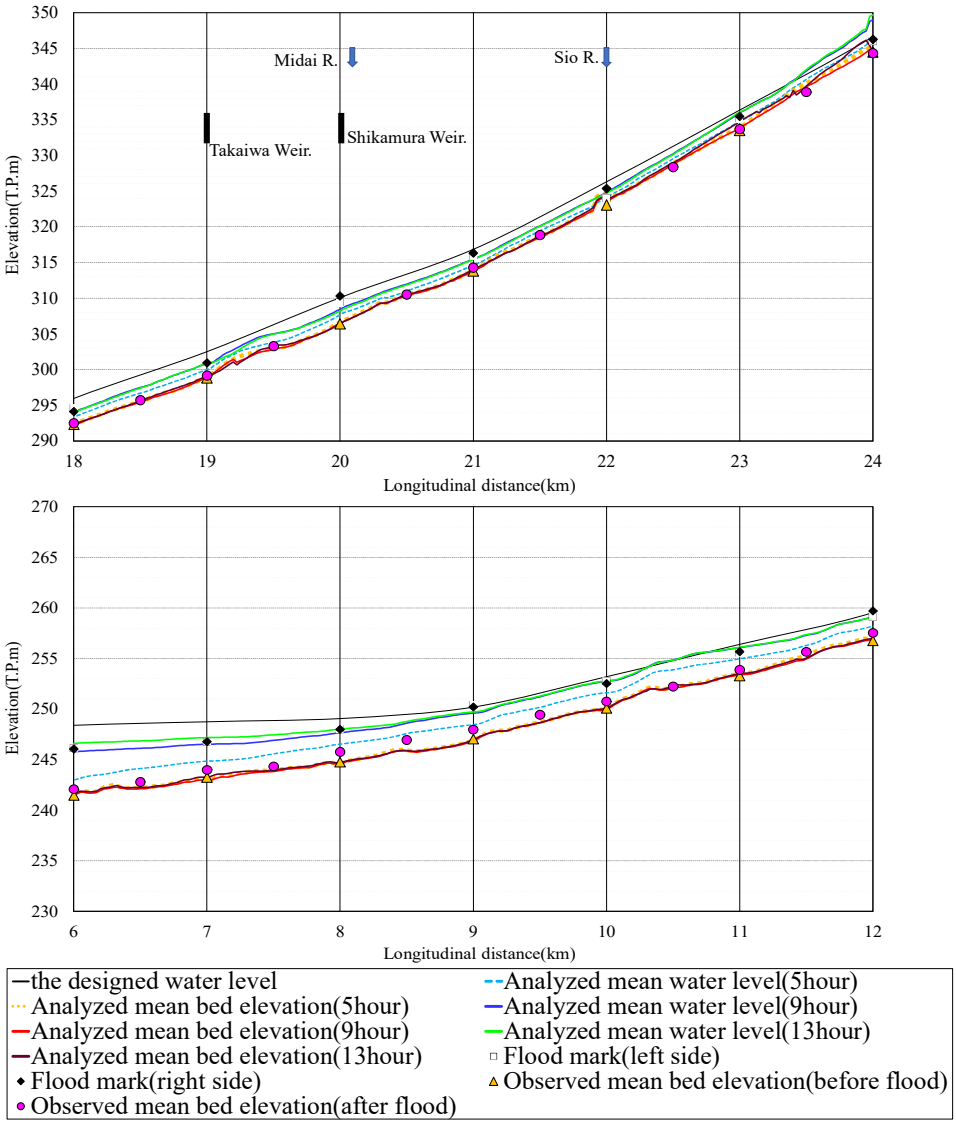

Figure 9. Longitudinal distribution of analyzed mean water level and analyzed mean bed level

23 km. In the reach between 24 km and 23 km, the calculated mean bed elevations became higher than the measured one, because the inflow sediment discharge from the upper reaches tend to deposit in this reach. Figure 10 indicates the longitudinal distribution of the amount of bed load and Figure 11 indicates the longitudinal distribution of the amount of suspended sediment. The amount of bed load of the grain size 100mm to 500mm gradually decreased from 23km to 13km at 9 hours (peak time). And the bed load with grain size of 8mm to 30mm shows a sharp decreasing in the longitudinal direction at peak time in the reaches between 23km to 21km and 13km to 12km. Therefore, the sediment depositions occurred in these reaches. From Figure 10 and Figure 11, the sediments with grain size of 0.5mm to 1.5mm were almost transported in states of suspensions. The suspended sediments decreased significantly in the reaches from 10km to 6km where the water surface gradients became mild after 9 hours (peak time).

Regarding the calculation results in the lower reaches, Figures 12(a), (b) and 12(c) show the depth-averaged suspended sediment concentration, existence ratio of particle size of 0.5mm to 1.5mm on bed surface, and contour of bed variation before and after the flood, respectively. At 5 hours (flood rising period), the suspended sediments from the upstream boundaries did not almost reach to the downstream of 10km point shown in Figure 11. Therefore, the suspended sediment concentration in this reach was low at this time shown in Figure 12(a). However, at 9 hours (peak time), the suspended sediments reached from upstream boundaries to the lower reach as shown in Figure 11. Thus the suspended load concentration increased after 9hours as shown in Figure 12(a). The amount of suspended sediment concentration decreased longitudinally in the reach from 10 km to 6 km due to mild water surface profiles and sediment depositions occurred as shown in Figure 12(c). Thus, the calculation results demonstrated that the bed materials on the bed surface became finer due to the deposition of suspended sediments in this reach. On the other hand, the calculated mean bed elevations were lower than the observed one. It is necessary to determine the inflow sediment discharge at the upstream end properly by using the developed bed variation analysis method.

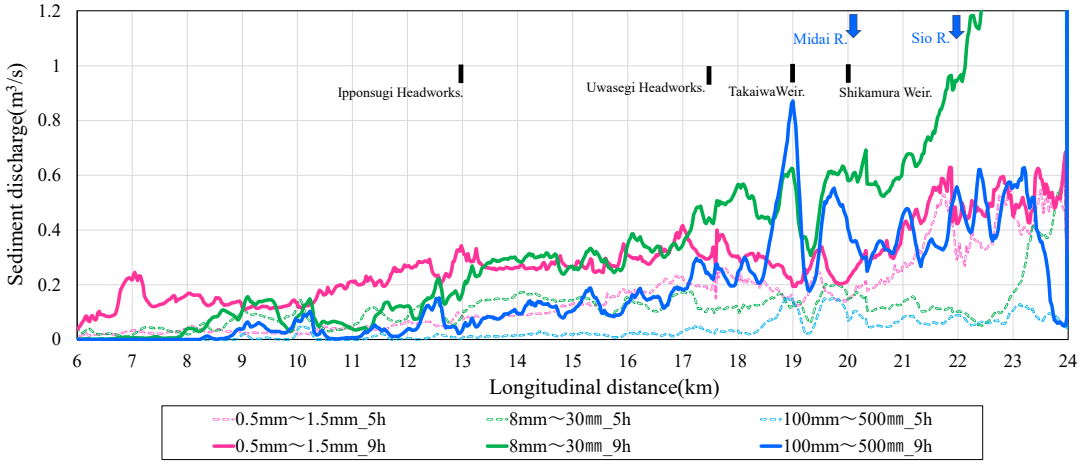

Figure 10. longitudinal distribution of amount of bed load

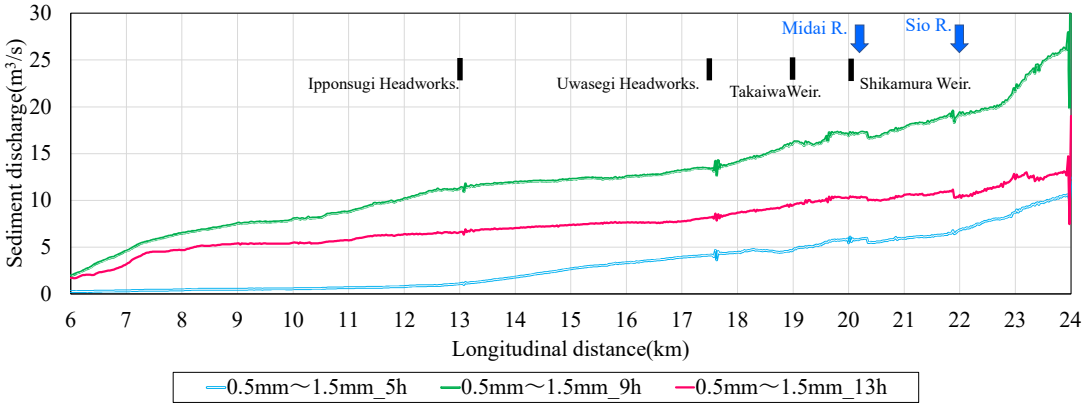

Figure 11. longitudinal distribution of amount of suspended load

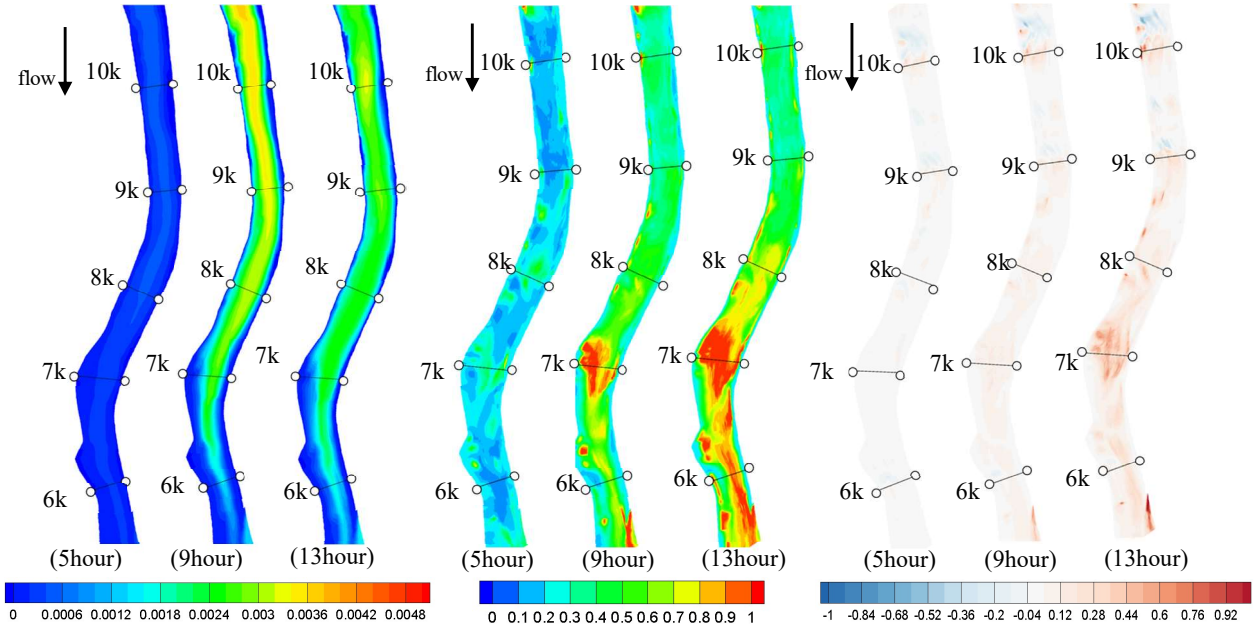

Depth-averaged suspended sediment concentration (%)

Existence ratio on bed surface (%)

Riverbed variation (m)

Figure 12(a). Depth-averaged suspended sediment concentration contour

Figure 12(b). Existence ratio on bed surface (0. 5mm～1.5mm)

Figure 12(c). Contour of bed variation before and after the flood

In upper reaches, Figure 13(a) shows existence ratio of particle sizes of 0.5mm to 1.5mm on bed surface at 5 hours. And Figures 13(b) to 13(d) show existence ratio of particle sizes of 0.5mm to 1.5mm, 8mm to 30mm, and 100mm to 500mm during the flood receding period (13 hours), respectively. The initial existence ratio on bed surface was that the particle size of 0.5mm to 1.5mm was 20%, 8mm to 30mm was 40% and 100mm to 500mm was 40%. At 5 hours in the flood rising period, the fine sediments deposited largely and the riverbed surface became finer. However, around 9 hours, the relatively coarse sediments whose sizes were 8mm to 30mm

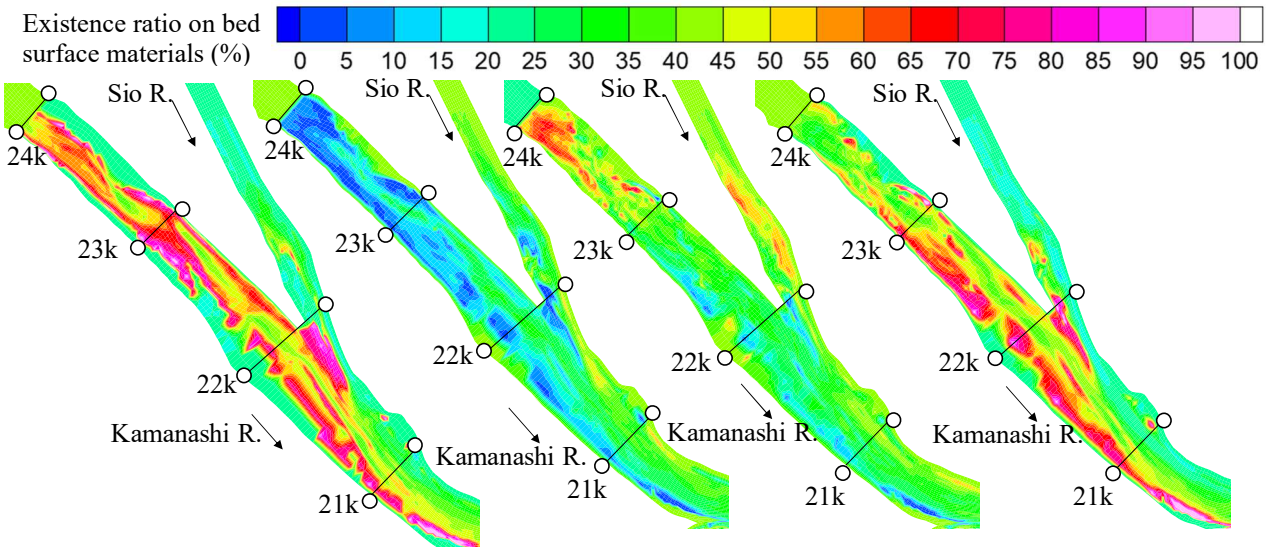

Figure 13. Existence ratio on bed surface materials (%)

(a). 0.5mm～1.5mm (5hour)

(b). 100mm～500mm (13hour)

(c). 8.0mm～ 30mm (13hour)

(d). 0.5mm～1.5mm (13hour)

flowed into this reach as shown in Figure 10, and the existence ratio of 8mm-30mm sizes increased to 50-60% as shown in Figure 13(c). The calculation results indicated that bed materials became coarser due to inflow sediment discharge. But these calculation results were smaller than the measured particle size distributions after the flood shown in Figure 2. It is necessary to examine effects of volume, shapes and phase shift of sediment graph of each particle sizes in relation to discharge hydrograph at the upper boundary on changes in riverbed and bed materials in the downstream reaches.

5. CONCLUSION

In this study, we developed a quasi-three-dimensional flood flow and bed variation analysis considering the non-equilibrium motion of boulders and gravel grains with a large amount of fine sediment motions. The developed method was applied to the 1982 flood in the Kamanashi River where a large amount of depositions and sorting of transported sediments occurred. The calculation results demonstrated that most of fine sediments were transported in states of suspensions to the lower reaches and it deposited in the reach where the water surface profiles became mild due to the Unose contraction reach and the confluence of the Fuefuki River. Thus, bed materials in the lower reaches became finer than sands shown in the observed data. In upper reaches, the calculated bed materials tended to become coarse around the time of the peak discharge.

However, the amount of sediment depositions in the calculations were much smaller than the observed one. And the analysis method was not able to calculate depositions of a particle size exceeding 100 mm observed in the upper reaches after the flood. Therefore, it was demonstrated that the determination method of the upstream boundary should consider the volume, shapes and phase shift of sediment graph of each particle sizes in relation to discharge hydrograph at the boundary.

REFERENCES

Gotoh, T and Fukuoka, S. (2019). Development and application of calculation method for amount of suspended sediment entrainment under non-equilibrium conditions of flows and sediment transports, *36th IAHR World Congress*, pp.1798-1807.

Ikeda, H. and Iseya, F. (1986). Longitudinal sorting process in heterogeneous sediment transport, *Proceedings of the japanese conference on hydraulics*, Vol.30, pp.217-222.

Osada, K., Fukuoka, S. and Ohgushi, H. (2013). Study of flood flow and gravel river bed variation analysis in the Satsunai River, Advances in River Sediment Research, *Proceedings of 12th International Symposium on River Sedimentation*, ISRS, pp.589-598.

Parker, G. (1991). Selective Sorting and Abrasion of River Gravel. I: Theory, *Journal of Hydraulic Engineering*, Vol.117, Issue2, pp.131-149.

Takemura, Y. and Fukuoka, S. (2019). Analysis of flows in undular and breaking hydraulic jumps by non-hydrostatic quasi three-dimensional model considering flow equations on boundary surfaces (Q3D-FEBS), *36th IAHR World Congress*, pp.2049-2055.